JOC Article
pubs.acs.org/joc

Neutral, Ion Gas-Phase Energetics and Structural Properties of Hydroxybenzophenones

Juan Z. Dávalos,*,† Andrés Guerrero,† Rebeca Herrero,† Pilar Jimenez,† Antonio Chana,† José Luis M. Abboud,† Carlos F. R. A. C. Lima,‡ Luís M. N. B. F. Santos,‡ and Alexsandre F. Lago§

†*Instituto de Quimica-Fisica "Rocasolano", CSIC, Serrano 119, 28006, Madrid, Spain,* ‡*Centro de Investigação em Química, Departamento de Química, Faculdade de Ciências da Universidade do Porto, P-4169-007 Porto, Portugal, and* §*Centro de Ciências Naturais e Humanas, Universidade Federal do ABC, 09210-170, Santo André, SP, Brazil*

jdavalos@iqfr.csic.es

Received January 22, 2010

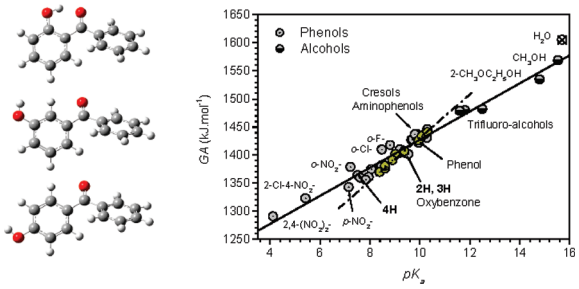

We have carried out a study of the energetics, structural, and physical properties of *o*-, *m*-, and *p*-hydroxybenzophenone neutral molecules, $C_{13}H_{10}O_2$, and their corresponding anions. In particular, the standard enthalpies of formation in the gas phase at 298.15 K for all of these species were determined. A reliable experimental estimation of the enthalpy associated with intramolecular hydrogen bonding in chelated species was experimentally obtained. The gas-phase acidities (*GA*) of benzophenones, substituted phenols, and several aliphatic alcohols are compared with the corresponding aqueous acidities (pK_a), covering a range of 278 $kJ \cdot mol^{-1}$ in *GA* and 11.4 in pK_a. A computational study of the various species shed light on structural effects and further confirmed the self-consistency of the experimental results.

1. Introduction

Benzophenone and its derivatives are of scientific and technological importance due to their interesting biological-therapeutic[1] and physical-chemical properties. They are widely used as synthons of chemical synthesis (i.e., 4-hydroxybenzophenone is an intermediate for the synthesis of the anticancer drug tamoxifen[2]), as active components of commercial sunscreens (safe protection against skin cancer and other forms of skin damage[3]), and as photoantioxidant additives of polymeric materials due to their capabilities to efficiently absorb a wide range of UV radiation (200−350 nm).[4]

Despite its fundamental and applied relevance, the thermodynamic properties of the benzophenone derivatives are incomplete. In order to obtain reliable data for these molecules, we have performed an experimental and theoretical investigation of structural effects on the intrinsic thermodynamical stability of neutral (Scheme 1) and anionic hydroxybenzophenones in the gas phase. We also have established a relationship of acidities between gaseous and dissolution phases of the studied species within a wider framework that includes phenol derivatives and aliphatic alcohols. In this context, we have used a number of experimental techniques

(1) (a) Khanum, S. A.; Venu, T. D; Shashikanth, S.; Firdouse, A. *Bioorg. Med. Chem. Lett.* **2004**, *14*, 5351. (b) Prabhakar, B. T.; Khanum, S. A.; Jayashree, K.; Salimath, B. P.; Shashikanth, S. *Bioorg. Med. Chem.* **2006**, *14*, 435.

(2) Top, S.; Kaloun, E. B.; Vessieres, A.; Leclercq, G.; Laios, I.; Ourevitch, M.; Deuschel, C.; McGlinchey, M. J.; Jaousen, G. *ChemBioChem.* **2003**, *4*, 754.

(3) (a) Maier, T.; Korting, H. C. *Skin Pharmacol. Physiol.* **2005**, *18*, 253. (b) Schallreuter, K. U.; Wood, J. M.; Farwell, D. W.; Moore, J.; Edwards, H. G. M. *J. Invest. Dermatol.* **1996**, *106*, 583. (c) Agin, P.; Anthony, F. A.; Hermansky, S. *LANCET* **1998**, *351*, 525.

(4) Dobashi, Y.; Kondou, J.; Ohkatsu, Y. *Polym. Degrad. Stab.* **2005**, *89*, 140 and references therein.

Published on Web 03/18/2010 DOI: 10.1021/jo100085b

SCHEME 1

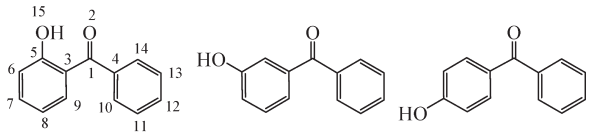

2H **3H** **4H**

such as differential scanning calorimetry (DCS), static bomb combustion calorimetry, Calvet microcalorimetry, Knudsen/Quartz effusion technique, Fourier transform ion cyclotron resonance mass spectrometry (FT-ICR), as well as quantum chemical calculations at the density functional theory (DFT) level. The present work is part of a systematic investigation of the energetics and structural properties of large conjugated organic molecules[5] with biological, medicinal, and industrial interest.

2. Results and Discussion

2.1. Combustion Calorimetry, Calvet Microcalorimetry, and Knudsen/Quartz Effusion Techniques. Enthalpies of Formation of the Neutral Molecules. The results from the combustion experiments are represented by reaction 1 and are shown in Table S2 of Supporting Information.

$$C_{13}H_{10}O_2(cr) + \frac{29}{2}O_2(g) \rightarrow 13CO_2(g) + 5H_2O(l) \qquad (1)$$

The standard (p^0 = 0.1 MPa) molar enthalpies of combustion, $\Delta_c H^0_m$(cr), and formation, $\Delta_f H^0_m$(cr), in the solid state (crystalline phase) at temperature T = 298.15 K are shown in Table 1. Their uncertainties are twice the final overall standard deviation of the mean and were estimated as outlined by Olofsson.[6] The values for the standard molar enthalpies of formation of H_2O (l) and CO_2 (g) at T = 298.15 K are −285.830 ± 0.042 kJ·mol^{-1} and −393.51 ± 0.13 kJ·mol^{-1}, respectively, taken from CODATA.[7]

The results and details of the sublimation experiments are summarized in Section S3 of Supporting Information. The standard molar enthalpy of sublimation $\Delta^g_{cr} H^0_m$ for **2H**, at T = 298.15 K, was calculated from the experimental value of $\Delta^{g,T}_{cr,298.15K} H^0_m$ at the temperature T of the microcalorimeter's hot zone, while $\Delta^g_{cr} H^0_m$ for **3H** and **4H** were determined from $\Delta^g_{cr} H^0_m$ (T_m) to the mean temperature (T_m) of its experimental range of measurement These results are summarized in Table 1. The lower (≈ 30 kJ·mol^{-1}) molar enthalpy of sublimation $\Delta^g_{cr} H^0_m$, of the **2H** isomer compared with the other two isomers is consistent with the existence of an intramolecular H-bond in **2H** (discussed in Section 2.3). In solid **3H** and **4H** the free hydroxyl group may establish typical intermolecular H bonds (see below), rising substantially the enthalpy of sublimation.

Taking into account the values of $\Delta_f H^0_m$(g) determined in this work, we can establish the following sequence of intrinsic thermodynamic stability of the hydroxybenzophenones: $\Delta_f H^0_m$(**2H**,g) < $\Delta_f H^0_m$(**4H**,g) < $\Delta_f H^0_m$(**3H**, g). The highest gas-phase thermochemical stability of the **2H** isomer is explained by the presence of the intramolecular H-bonding that exerts an important stabilizing effect. Among the other isomers, **4H** is 6.5 kJ·mol^{-1} more stable than **3H**. Such a difference can be explained by the contribution of a highly stabilized charge-transfer type valence bond structure on *para*-derivative **4H**, which is not possible in the case of the *meta*-derivative **3H**.

TABLE 1. Experimental Determination of Standard Molar Enthalpies of Combustion, Formation (in Solid and Gaseous States), and Sublimation at T = 298.15 K and p^0 = 10^5 Pa[a]

	$\Delta_c H^0_m$(cr)	$\Delta_f H^0_m$(cr)	$\Delta^g_{cr} H^0_m$	$\Delta_f H^0_m$(g)
2H	−6295.3 ± 3.4	−245.7 ± 3.8	97.9 ± 1.9	−147.8 ± 4.3
3H	−6397.4 ± 3.4	−247.3 ± 4.0	131.7 ± 0.9	−115.6 ± 3.9
4H	−6292.9 ± 3.3	−252.4 ± 3.3	130.3 ± 1.0	−122.1 ± 3.8

[a]All values are given in kJ·mol^{-1}.

TABLE 2. Experimental Determination of the Gas-Phase Acidity of 2H[a]

$A_{ref}H$	$GA(A_{ref}H)^{b,c}$	$RT \ln K_p{}^b$	GA(**2H**)^b
p-chlorophenol	1407.9 ± 8.4	4.2	1403.7
pivalic acid	1413.4 ± 8.4	10.5	1402.9
2-methyl propanoic acid	1418.4 ± 8.4	15.9	1402.5
m-chlorophenol	1402.9 ± 8.4	−1.7	1404.6
m-fluorophenol	1410.8 ± 8.4	8.0	1402.5
average			1403.3 ± 1.8

[a]All values in are given kJ·mol^{-1}. [b]Defined in Section 4.4. [c]Taken from ref 8.

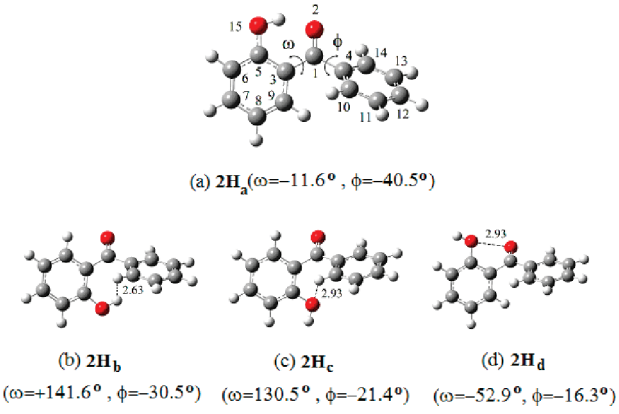

(a) **2H$_a$**(ω=–11.6°, ϕ=–40.5°)

(b) **2H$_b$** (ω=+141.6°, ϕ=–30.5°) (c) **2H$_c$** (ω=130.5°, ϕ=–21.4°) (d) **2H$_d$** (ω=–52.9°, ϕ=–16.3°)

FIGURE 1. Molecular geometry for stable conformers of **2H** optimized at the B3LYP/6-311++G(3df,2p) level. Distances are given in angstroms.

2.2. Ion Energetics. Acidity of 2-Hydroxybenzophenone. The K_p values were taken as the average of six different experiments involving different ratios of the neutral bases pressures. Experimental results are summarized in Table 2. The estimated uncertainties, ±1.8 kJ·mol^{-1}, are twice the standard deviation of the mean. However, although this value is satisfactory, the accuracy of the $GA(A_{ref}H)$ values is given as ±8.4 kJ·mol^{-1},[8] and thus we consider the same uncertainty for our result: GA(**2H**) = 1403.3 ± 8.4 kJ·mol^{-1}.

2.3. Structures, Hydrogen-Bond, and Thermochemistry Properties of Neutral Molecules. The computed energies and enthalpies for the stable conformations of the hydroxybenzophenones, their transition states (TSs), activation

(5) Lago, A. F.; Jimenez, P.; Herrero, R.; Dávalos, J. Z.; Abboud, J.-L. M. *J. Phys. Chem. A* **2008**, *112*, 3201.

(6) Olofsson, G. Assignment of Uncertainties. In *Combustion Calorimetry*; Sunner, S., Mänson, M., Eds.; Pergamon Press: Oxford, 1979; Chapter 6.

(7) CODATA. Recommended key values for thermodynamics. 1975. *J. Chem. Thermodyn.* **1976**, *8*, 603.

(8) *NIST Chemistry Webbook*; NIST Standard Reference Database, http://webbook.nist.gov.

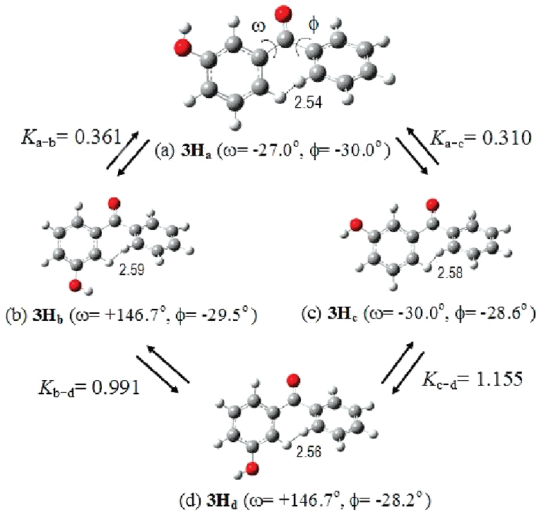

FIGURE 2. Molecular geometry for stable conformers of **3H** optimized at the B3LYP/6-311++G(3df,2p) level. Distances are given in angstroms.

barriers, and equilibrium molar fractions are described in detail in Section S4 of Supporting Information.

Structure of 2-Hydroxybenzophenone (2H). Figure 1 shows the different conformers **2H$_a$**, **2H$_b$**, **2H$_c$**, and **2H$_d$**. The most stable conformer of **2H** was found to be the chelated form (**2H$_a$**). For the sake of simplicity the labeling is shown only for **2H$_a$** (see Scheme 1 and Figure 1a). The dihedral angle $\omega = D(O_2-C_1-C_3-C_5)$ [or angle $\phi = D(O_2-C_1-C_4-C_{14})$] is formed by the plane containing the substituted [or unsubstituted] benzene ring and the plane of the rest of the molecule.

Rotation of the phenolic moiety of **2H$_a$** around the C_3-C_1(O) bond leads to structure **2H$_b$**, in which the chelation [OH···O(C)] and also the interaction between the OH group and the unsubstituted phenyl moiety is absent. In terms of enthalpy, both conformers differ by 31.4 kJ·mol^{-1} (change in enthalpy for the process **2H$_a$** → **2H$_b$**) with an activation barrier of 34.1 kJ·mol^{-1}. The equilibrium molar fraction of **2H$_b$** can be estimated (from the calculated Gibbs free energies) at ca. 8.9×10^{-6}, indicating that, under normal conditions, the formation of this conformer is quite unfavorable and rather slow. Rotation of the hydroxyl group in **2H$_b$** around the C_5-OH bond leads to structure **2H$_c$**, while rotation of the same group in structure **2H$_a$** leads to structure **2H$_d$**, wherein chelation is also destroyed. The relative stability of **2H$_c$** and **2H$_d$** reveals that these conformers are, respectively, 36.9 and 41.3 kJ·mol^{-1} less stable than **2H$_a$** (see Section S4 of Supporting Information). The corresponding equilibrium molar fraction (estimated at ca. 1.8×10^{-6} and 4.5×10^{-7}, respectively) indicates that **2H$_c$** and **2H$_d$** contributions to the total population of **2H** is not significant.

Rotation of the unsubstituted benzene moiety of **2H$_a$** ($\omega = -11.6°$, $\phi = -40.5°$) upon the C_4-C_1(O) bond leads to the formation of its conformer **2′H$_a$** ($\omega = 11.6°$, $\phi = 40.5°$). This takes place for all the hydroxybenzophenones (also including anionic species).

Structure of 3-hydroxybenzophenone (3H). Figure 2 shows the four conformers of **3H**, **3H$_a$** being the most stable. Rotation of the phenolic moiety of **3H$_a$** around the C_3-C_1(O) bond leads to structure **3H$_b$**, while rotation of the hydroxyl group (around the C_5-OH bond) in **3H$_b$** leads to structure **3H$_d$**. Rotation of the same group in structure **3H$_a$** leads to structure **3H$_c$**. Relative stabilities of **3H$_b$**, **3H$_c$**, and **3H$_d$** are similar, while **3H$_a$** is almost 3 kJ·mol^{-1} more stable than the others. The activation barrier is the same (9.8 kJ·mol^{-1}) for transitions **3H$_a$**−**3H$_b$** and **3H$_a$**−**3H$_c$**, while it is 13.5 kJ·mol^{-1} for transition **3H$_a$**−**3H$_d$**. The equilibrium constants (or equilibrium molar fractions) K_{a-j} related to the equilibrium 3H$_a$ ⇄ **3H$_j$** are 0.361, 0.310, and 0.358 for each rotamer j = b, c, d, respectively. On the basis of those K_{a-j} it follows that, at ca. 298.15 K, a sample of gaseous **3H** is a dynamic equilibrium mixture of approximately 49.3%, 17.8%, 15.3%, and 17.6% of **3H$_a$**, **3H$_b$**, **3H$_c$**, and **3H$_d$**, respectively.

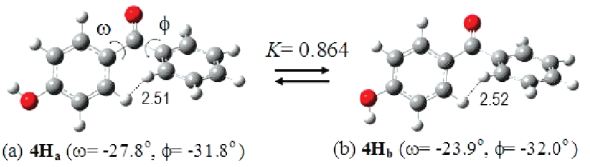

FIGURE 3. Molecular geometry for stable conformers of **4H** optimized at the B3LYP/6-311++G(3df,2p) level. Distances are given in angstroms.

Structure of 4-Hydroxybenzophenone (4H). This compound has two conformers with similar stability (Figure 3). Rotation of the hydroxyl group in **4H$_a$** around the C_3-OH bond, overcoming an activation barrier of 14.6 kJ·mol^{-1}, leads to structure **4H$_b$**. The equilibrium constant pertaining to the reaction, **4H$_a$** ⇄ **4H$_b$**, is 0.864 (see Figure 3 and Section S4 of Supporting Information). At 298.15 K, **4H** is expected to be an equilibrium mixture of **4H$_a$** (53.7%) and **4H$_b$** (46.3%).

The theoretical optimized geometries for the structures of hydroxybenzophenones are in good agreement with the available experimental XRD data (see Table S7 of Supporting Information). The observed deviations can be attributed to the fact that the experimental structure is determined in the solid state, whereas the calculations refer to the gas phase. It is important to mention that experimental XRD structures of **3H** and **4H** are related with their **3H$_b$** and **4H$_b$** conformers, respectively. These conformers can form "infinite chains" by intermolecular H-bonding associated with O−H···O=C interactions (see stable dimers of **3H** and **4H** in Supporting Information).

Intramolecular H-Bonding (*HB*) in 2H$_a$. The associated enthalpy with intramolecular H-bonding interaction in chelated **2H$_a$** was estimated by the use of purely experimental data as the enthalpy of homodesmotic reaction 2, $\Delta_r H^0(2) = HB = 23.6 \pm 5.7$ kJ·mol^{-1}. In this reaction, only standard enthalpies of formation of chelated **2H$_a$** (*ortho*) and nonchealated **4H** (*para*) are required (known as the "*ortho-para*" method). The *ortho-para* method is probably the best way to quantify the intramolecular H-bonding.[9] The previous experimental result is quite consistent and comparable with the following computational study results:

(i) The theoretical enthalpy of the homodesmotic reaction 2 is $\Delta_r H^0(2)_{theor} = 22.9$ kJ·mol^{-1}.

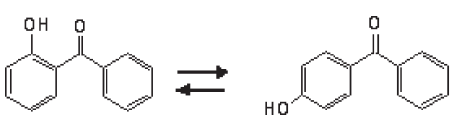

(2)

(ii) The enthalpy of the isodesmic reaction 3 obtained from theoretical and purely experimental data are 27.3 and

(9) Estácio, S. J. A. G.; Cabral do Couto, P.; Costa Cabral, B. J.; Minas da Piedade, M. E.; Martinho Simoes, J. A. *J. Phys. Chem. A* **2004**, *108*, 10834.

18.4 ± 5.7 kJ·mol^{-1}, respectively. This reaction is associated with intramolecular H-bond breaking/forming in **2H$_a$**. The experimental values rely on known $\Delta_f H^0_m$(g) values of benzene (82.93 ± 0.50 kJ·mol^{-1}), benzophenone (49.9 ± 3.0 kJ·mol^{-1}), and phenol (96.36 ± 0.59 kJ·mol^{-1}), taken from NIST Standard Reference Database;[8] the $\Delta_f H^0_m$(g) value of **2H$_a$** is determined in this work.

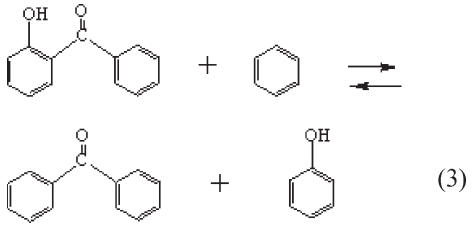

(3)

(iii) In the homodesmotic reaction 4, the most stable conformer **2H$_a$** is compared to the less stable **2H$_b$** where the intramolecular H-bond is absent. We find that the enthalpy of this reaction is $\Delta_r H^0(4) = 31.4$ kJ·mol^{-1}. Considering the less stable conformers **2H$_c$** and **2H$_d$**, the corresponding $\Delta_r H^0(4)$ is 36.9 and 41.3 kJ·mol^{-1}, respectively. These values are higher than the enthalpy associated with intramolecular H-bonding interaction, probably due to a weaker conjugation in **2H$_b$**, **2H$_c$**, and **2H$_d$** caused by the lower degree of planarity of the phenol moiety relative to C=O.

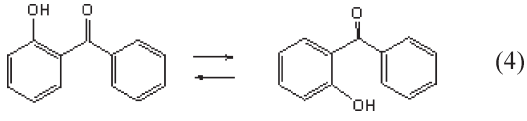

(4)

(iv) The enthalpies of the isodesmic reaction 5, $\Delta_r H^0(5)$, obtained from theoretical and purely experimental data are 9.4 and 11.7 ± 7.0 kJ·mol^{-1}, respectively. In this reaction we compared the enthalpies associated with intramolecular H-bonding interaction (*HB*) in both, **2H$_a$** and oxybenzone chelated compounds. The difference between their corresponding experimental *HB* values is $\Delta HB = 6.5$ kJ·mol^{-1}, and it is comparable to $\Delta_r H^0(5)$ values. The greater stability of oxybenzone molecule can be attributed to the presence of the stabilizing *p*-methoxy electron-donating group in this molecule.

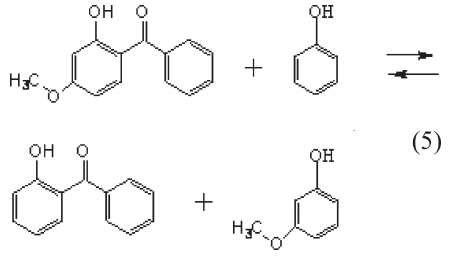

(5)

The wavenumber σ(OH) for the OH stretching vibration is considered as a sensitive property to hydrogen-bond interactions.[10] The calculated σ(OH) value for chelated **2H$_a$** is 3332.8 cm^{-1}, while σ(OH) for nonchelated species such as **2H$_b$**, **2H$_c$**, and **2H$_d$** conformers and **3H** and **4H** isomers are between 3776 and 3837 cm^{-1} (Table S4 of Supporting Information). Thus, the average red-shift of the OH stretching vibration in chelated **2H$_a$** relative to nonchelated conformers and isomers is $\Delta\sigma$(OH) = 495 ± 20 cm^{-1}, meaning an approximately 13% effect. These results are comparable to the following: $\Delta\sigma$(OH) = 500 cm^{-1} obtained from calculated σ(OH) of oxybenzone chelated and their conformers and nonchelated isomers[5] and $\Delta\sigma$(OH) = 475 cm^{-1} obtained from experimental data on the gas-phase IR spectra of phenol and **2H**.[11]

(v) The value for σ(OH) and distance $d(O_2-O_{15})$ of **2H$_a$** (Table S5 of Supporting Information) are well within the range of the linear correlation between σ(OH) and the O···O distance for chelated compounds reported in classical studies.[12] Furthermore, the values of $d(H-O_2)$ and $d(O_2-O_{15})$ are also consistent with the empirical relationship of these geometric parameters for a wide variety of H-bond systems obtained by Olovsson and Jönsson[13] from neutron diffraction studies.

Combining σ(OH) value with geometric data, such as H···O$_2$ distance (1.6784 Å) or O−H···O angle (146.9°), and enthalpy of reaction 2, allows the classification of the H-bond in **2H$_a$** as a "moderate"[14] or "conventional-strong"[15] bond, which has an electrostatic character and belongs to the most common H-bond type found in nature.

The experimental and computational results obtained in this work for the strength of the H-bond are in good agreement with the results published in a recent work by Bernardes and Minas da Piedade[16] where they study the energetics of the intramolecular H-bond in series of HOC$_6$H$_4$C(O)R (R = substituents) derivatives.

2.4. Structures, Energetics, and Intrinsic Gas-Phase Acidity of Hydroxybenzophenone Anions ($C_{13}H_9O_2^-$). The computed energies, enthalpies, and structures of the possible anionic hydroxybenzophenone stable conformers (formed by OH deprotonation), their transition states (TSs), activation barriers, and equilibrium molar fractions are described in Supporting Information (Section S4) and Figures 4−6.

On the protonation of **2**$^-$, it is important to mention that ion selection experiments[17] show the extremely clean reversibility of reaction 8, its explanation being consistent with the protonation at O$_{15}$. However, is the protonation at O$_2$ (oxygen of C=O) possible? The collisions between **2**$^-$ and A$_{ref}$H may lead in principle to protonation on O$_2$ and O$_{15}$. In fact, the species obtained by protonation at O$_2$ (full details are given in Supporting Information, Section S6) is a minimum on the potential energy surface (PES) but is significantly less stable than the species obtained by protonation on O$_{15}$ (i.e., 116.2 kJ·mol^{-1} less stable than **2H$_a$**). These results

(10) Pimentel, G. C.; McClellan, A. L. *The Hydrogen Bond*; Pauling, L., Ed.; W. H. Freeman and Company: San Francsico and London, 1960.

(11) Lampert, H.; Mikenda, W.; Karpfen, A. *J. Phys. Chem.* **1996**, *100*, 7418.

(12) (a) Dearden, J. C. *Nature* **1965**, *206*, 1147. (b) Nakamoto, K.; Margoshes, M.; Rundle, R. E. *J. Am. Chem. Soc.* **1955**, *77*, 6480.

(13) Olovsson, I.; Jönsson, P.-G. In *Hydrogen Bond II: Structure and Spectroscopy*; Schuster, P., Zundel, G., Sandorfy, C., Eds.; North Holland Publishing Co.: Amsterdam, 1976; Chapter 8, p 393.

(14) Jeffery, G. A. *An Introduction to Hydrogen bonding*; Oxford University Press: New York 1997.

(15) Desiraju, G. R.; Steiner, T. *The Weak Hydrogen Bond in Structural Chemistry and Biology*, IUCr Monographs on Crystallography 9; Oxford University Press: New York, 1999.

(16) Bernardes, C. E. S.; Minas da Piedade, M. E. *J. Phys. Chem. A* **2008**, *112*, 10029.

(17) Lehman, T. A.; Bursey, M. M. *Ion Cyclotron Resonance Spectrometry*; John Wiley & Sons: New York, 1976; p 175.

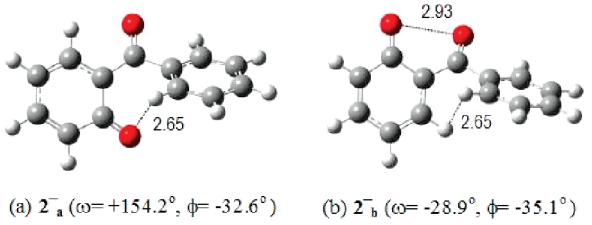

FIGURE 4. Molecular geometry for stable conformers of anion $\mathbf{2}^-$ optimized at the B3LYP/6-311++G(3df,2p) level. Distances are given in angstroms.

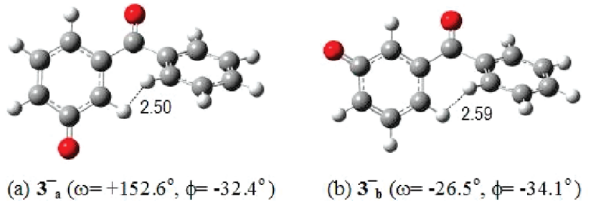

FIGURE 5. Molecular geometry for stable conformers of anion $\mathbf{3}^-$ optimized at the B3LYP/6-311++G(3df,2p) level. Distances are given in angstroms.

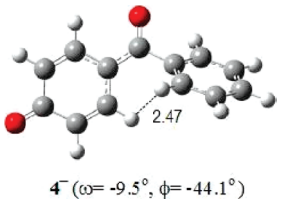

FIGURE 6. Molecular geometry for stable anion $\mathbf{4}^-$ optimized at B3LYP/6-311++G(3df,2p) level. Distance is given in angstroms.

are also given for other isomers, where the species obtained by protonation at O_2 of $\mathbf{3}^-$ and $\mathbf{4}^-$ are 188.7 and 77.1 kJ·mol^{-1} less stable than $\mathbf{3H_a}$ and $\mathbf{4H_a}$, respectively. Therefore, only the protonation on O_{15} prevails.

Structure of 2-Hydroxybenzophenone Anions ($\mathbf{2}^-$). The optimized geometries of the $\mathbf{2}^-$ anions show basically two stable conformers ($\mathbf{2}^-_\mathbf{a}$ and $\mathbf{2}^-_\mathbf{b}$, Figure 4). Both of them resemble the neutral rotamers $\mathbf{2H_b}$ (or $\mathbf{2H_c}$) and $\mathbf{2H_a}$ (or $\mathbf{2H_d}$), respectively. The geometrical parameters such as the distance $d(O_2-C_1)$ (~1.23 Å, Table 4) of the C=O group remains practically constant, while the distance $d(O_{15}-C_5)$ is significantly shortened (by approximately 0.09 Å) upon deprotonation. In terms of enthalpy, $\mathbf{2}^-_\mathbf{a}$ and $\mathbf{2}^-_\mathbf{b}$ differ by 21.2 kJ·mol^{-1}, where $\mathbf{2}^-_\mathbf{a}$ is found as the most stable. The derived activation barrier for the transition $\mathbf{2}^-_\mathbf{a} \rightarrow \mathbf{2}^-_\mathbf{b}$ is 27.8 kJ·mol^{-1}, and the equilibrium constant K of the reaction $\mathbf{2}^-_\mathbf{a} \rightleftarrows \mathbf{2}^-_\mathbf{b}$ is 3.4×10^{-4}. From this value, we can deduce that $\mathbf{2}^-_\mathbf{b}$ is not present in significant amount.

Structure of 3-Hydroxybenzophenone Anions ($\mathbf{3}^-$). As in the previous case, the optimized geometry of the $\mathbf{3}^-$ anions show basically two stable conformers ($\mathbf{3}^-_\mathbf{a}$ and $\mathbf{3}^-_\mathbf{b}$, Figure 5) resembling also the neutral rotamers $\mathbf{3H_b}$ (or $\mathbf{3H_d}$) and $\mathbf{3H_a}$ (or $\mathbf{3H_c}$), respectively. The distance $d(O_2-C_1)$ of the C=O group in $\mathbf{3}^-$ anions is a little longer (by approximately 0.007 Å) than in the neutral **3H**, while the distance $d(O_{15}-C_5)$ is significantly shortened (by approximately 0.103 Å) upon deprotonation. From our theoretical calculation, we find that $\mathbf{3}^-_\mathbf{a}$ is only 3.0 kJ·mol^{-1} more stable than $\mathbf{3}^-_\mathbf{b}$, with an activation barrier (transition $\mathbf{3}^-_\mathbf{a} \rightarrow \mathbf{3}^-_\mathbf{b}$) of 12.9 kJ·mol^{-1}. The equilibrium constant K of the reaction $\mathbf{3}^-_\mathbf{a} \rightleftarrows \mathbf{3}^-_\mathbf{b}$ is 0.2906. This value indicates that gaseous 3-hydroxybenzophenone anions at 298.15 K would be an equilibrium mixture of approximately 77.5% and 22.5% of $\mathbf{3}^-_\mathbf{a}$ and $\mathbf{3}^-_\mathbf{b}$, respectively.

TABLE 3. Experimental Values of Acidity (GA) and Deprotonation Enthalpy ($\Delta_{acid}H^0$) of Hydroxybenzophenones and the Standard Molar Enthalpies of Formation ($\Delta_fH^0_m$(g)) of Their Corresponding Anions

	GA			$\Delta_{acid}H^0$	$\Delta_fH^0_m$(g)
2H	1403.3 ± 8.4[a]	$\mathbf{2}^-$		1438.1 ± 8.4[a]	−243.9 ± 9.4[a]
3H	1400.0 ± 8.4[b]	$\mathbf{3}^-$		1428.0 ± 8.4[b]	−223.8 ± 9.3[a]
4H	1364.0 ± 8.4[b]	$\mathbf{4}^-$		1393.0 ± 8.4[b]	−265.3 ± 9.2[a]
oxybenzone	1402.1 ± 8.4[c]	oxybenzone anion		1437.5 ± 8.4[c]	−402.3 ± 9.8[c]

[a]Determined in this work. [b]Taken from ref 8. [c]Taken from ref 5.

TABLE 4. Distances and NBO Charge Distributions of Anionic Species

	distance (Å)			natural charges (electronic units)	
anion	O_2-C_1	$O_{15}-C_5$	C_1-C_3	O_2	O_{15}
$\mathbf{2}^-_\mathbf{a}$	1.2349	1.2550	1.4638	−0.638	−0.734
$\mathbf{2}^-_\mathbf{b}$	1.2259	1.2462	1.4613	−0.587	−0.697
$\mathbf{3}^-_\mathbf{a}$	1.2249	1.2627	1.4804	−0.602	−0.778
$\mathbf{3}^-_\mathbf{b}$	1.2232	1.2610	1.4810	−0.593	−0.772
$\mathbf{4}^-$	1.2401	1.2523	1.4419	−0.660	−0.723

Structure of 4-Hydroxybenzophenone Anion ($\mathbf{4}^-$). The optimized geometry of the $\mathbf{4}^-$ anion shows only one stable species ($\mathbf{4}^-$, Figure 6). As in the $\mathbf{3}^-$ case, the distance $d(O_2-C_1)$ of the C=O group in $\mathbf{4}^-$ anion is longer, by approximately 0.021 Å, than in the neutral **4H**, while the distance $d(O_{15}-C_5)$ is shortened, by approximately 0.108 Å, upon deprotonation.

Intrinsic Gas-Phase Acidity and Stability of Hydroxybenzophenone Anions. The calculated theoretical gas-phase acidity of **2H**, GA_{theor}(**2H**), obtained considering the conformers contributions (Table S4 of Supporting Information) are 1394.1 and 1398.2 kJ·mol^{-1} for the 6-311++G(d,p) and 6-311+G(3df,2p) basis sets employed, respectively. Although both values have an acceptable agreement with the experimental value, GA(**2H**) = 1403.3 ± 8.4 kJ·mol^{-1}, it is remarkable that the agreement of the second one is better. From the experimental GA(**2H**) value we can obtain, using the computed entropy change from values given in Table S7 of Supporting Information, the deprotonation enthalpy (defined in Section 4.4) $\Delta_{acid}H^0$(**2H**) = 1438.1 ± 8.4) kJ·mol^{-1}. This value allows us to estimate (using eq 9 and the heat of formation of H^+ taken from JANAF[18]) the standard heat of formation in the gas phase of anion $\mathbf{2}^-$, $\Delta_fH^0_m(\mathbf{2}^-,g)$ = −243.9 ± 9.4 kJ·mol^{-1}. We used the same procedure to estimate the standard heat of formation of $\mathbf{3}^-$ and $\mathbf{4}^-$ species. Acidities (GA), deprotonation enthalpies ($\Delta_{acid}H^0$) of neutral hydroxybenzophenones, and heats of formation of their corresponding anions are summarized in Table 3.

Experimental GA values for **2H**, **3H**, and oxybenzone are practically the same (Table 3), while for **4H** it is almost 38 kJ·mol^{-1} lower. These values are related to the stability of both neutral and anionic species. The enhanced acidity of **4H** can be attributed to a resonance stabilization effect[19] of its

(18) Chase, M. W., Jr. *NIST-JANAF Thermochemical Tables*, 4th ed.; American Institute of Physics: New York, 1998.
(19) Silva, P. J. *J. Org. Chem.* **2009**, *74*, 914 and references therein.

anion $\mathbf{4}^-$. This anion is 21.4 and 41.5 kJ·mol^{-1} more stable than $\mathbf{2}^-$ and $\mathbf{3}^-$ anions, respectively. The influence of resonance effect is related to the charge distribution of the deprotonated species, and a substantial part of the negative charge of anions spreads over the entire ion, concentrating on atoms O_2 and particularly O_{15}, as is confirmed by the NBO (calculated at the B3LYP/6-311++G(32df,2p) level) charge distribution calculations (see Table 4). The charge-dispersal stabilizing effect on the anions can be established in terms of absolute values of difference of natural charges between O_2 and O_{15} (ΔQ). The sequence ΔQ ($\mathbf{4}^-$) < ΔQ ($\mathbf{2}^-$) < ΔQ ($\mathbf{3}^-$) is the same as that for the corresponding $\Delta_f H^0_m$ of the anions studied. Thus, the increased stability of anion $\mathbf{4}^-$ over $\mathbf{2}^-$ and $\mathbf{3}^-$ anions would imply a greater homogeneity of its charge distribution. The same can be established for others anion conformers of $\mathbf{2}^-$ and $\mathbf{3}^-$, ΔQ ($\mathbf{2}^-_a$) < ΔQ ($\mathbf{2}^-_b$) and ΔQ ($\mathbf{3}^-_a$) $\approx \Delta Q$ ($\mathbf{3}^-_b$) being in good agreement with their corresponding $\Delta_f H^0_m$(g) values. These facts are also reflected in the geometry changes upon deprotonation of hydroxybenzophenones; in particular, the shortening of bond lenghts of $O_{15}-C_5$ and C_1-C_3 are significant. It is remarkable that the sequence of distance $d(C_1-C_3)$ of the anions (see Table 4) is the same as that for their corresponding stabilities, $\Delta_f H^0_m$(g): $d(\mathbf{4}^-) < d(\mathbf{2}^-) < d(\mathbf{3}^-)$.

In the case of the chelated species such as oxybenzone and **2H**, we can considerer a process (reaction 6) similar to reaction 5 involving the corresponding anionic species:

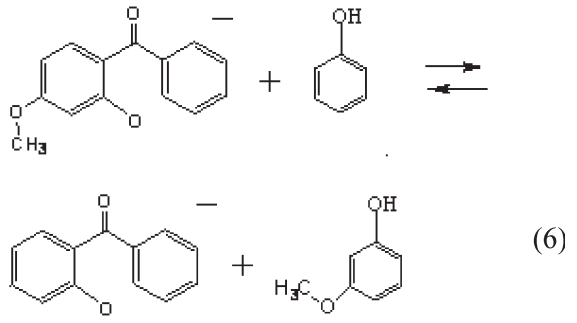

(6)

Using the experimentally based data reported above and in ref 5, we obtain $\Delta_r H^0_m(6) = 14.4$ kJ·mol^{-1}, close to $\Delta_r H^0_m(5)$ but almost 8 kJ·mol^{-1} higher than the difference in *HB* values of their corresponding neutrals. This result confirms and quantifies the stabilizing effect of *p*-methoxy group in the oxybenzone.

2.5. Relationship between the Gas-Phase Acidity (*GA*) of Hydroxybenzophenones, Phenols (and Also Several Aliphatic Alcohols), and Their pK_a Values in Water Solution. Experimental pK_a values in water solution of hydroxybenzophenones[20] are in the acidity range of phenols and increase as pK_a **4H** (7.51) < pK_a **3H** (9.0) < pK_a **2H** (9.44). This trend is identical to that observed with the acidity in the gas phase, *GA*.

The relationship between *GA* and aqueous acidity (pK_a) of 44 compounds (including benzophenones; *o*-, *m*-, *p*-phenol derivatives; trifluoro-alcohols; methoxy-ethanol, and methanol) is shown in Figure 7 (the experimental values were taken from refs 8, 21, 22 and the present work).

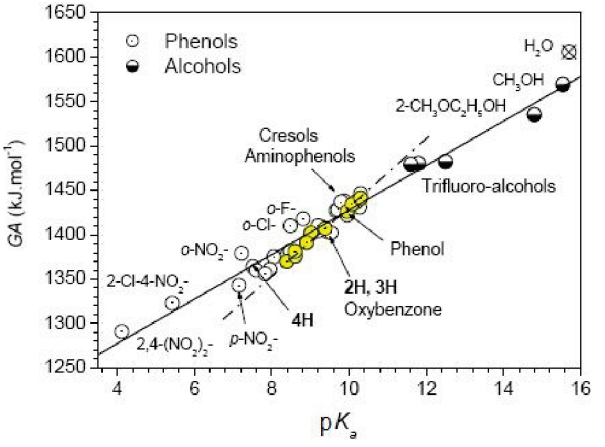

FIGURE 7. Comparison between experimental gas-phase (*GA*) and aqueous (pK_a) acidities of benzophenones, phenol derivatives, and several aliphatic alcohols.

The linear correlation obtained is

$$GA = 25.025\mathrm{p}K_a + 1177.43(\mathrm{kJ\cdot mol^{-1}}) \qquad (7)$$

where the average deviation of calculated *GA* is ± 9.05 kJ·mol^{-1} covering a range of 278 kJ·mol^{-1} (the pK_a range is almost 11.4) and the correlation coefficient is 0.977. The slope of the correlation line gives the substituent effect attenuation factor for aqueous solvent. It is, in comparative terms of standard Gibbs free energies, 4.5 times larger in the gas phase than in aqueous solution. Atenuation factors of 5−7 were found for *m*-, *p*-substituted phenols and benzoic acids[22,23] and for substitued pyridines were 2−4.[24] It is important to mention that Taft et al.[22] studied the effects of selected *m*- and *p*-phenol subtituents in the gas phase and their correlation with the substituent effects in water solution, covering an acidity range of 73.6 kJ·mol^{-1} (pK_a range roughly 3.2). This linear relationship (with slope of 6.56 and shown, in Figure 7, with a dotted line) of very satisfactory precision was limited basically to *non*-hydrogen bond acceptor substituents. The factor of attenuation was attributed to the combined effect of strong specific solvatation of the phenoxide ions, the specific solvation of phenols, and the dielectric constant factor for nonspecific solvation. McMahon and Kebarle[23] also found a linear correlation of gas-phase and aqueous acidities of substituted phenols, with a slope of 6.8. This factor is considered to be unusually large by the authors.

Although it is known that *ortho*-substituted benzene derivatives exhibit anomalous behavior in structure−reactivity relationships, we include several derivatives in this work. However, it is remarkable that points such as *o*-NO_2, -F and -Cl phenols deviate significantly upward of calculated *GA* by almost 20 kJ·mol^{-1}. Other substituted phenols (*m*- and *p*-NO_2, -CN, -CF_3 substituents) also fall outside the correlation line with a deviation higher than 9 kJ·mol^{-1}. This fact is

(20) (a) Castro, G. T.; Giordano, O. S.; Blanco, S. E. *J. Mol. Struct. (Theochem)* **2003**, *626*, 167. (b) Bhasikuttan, A. C.; Singh, A. K.; Palit, D. K.; Sapre, A. V.; Mittal, J. P. *J. Phys. Chem. A* **1999**, *103*, 4703.

(21) pK_a data compiled by Williams, R.: http://www.chem.tamu.edu/rgroup/connell/links.

(22) Fujio, M.; McIver, R. T., Jr.; Taft, R. W. *J. Am. Chem. Soc.* **1981**, *103*, 4017.

(23) McMahon, T. B.; Kebarle, P. *J. Am. Chem. Soc.* **1997**, *99*, 2222.

(24) Taagepera, M.; Henderson, W. G.; Brownlee, R. T. C.; Beauchamp, J. I.; Holtz, D.; Taft, R. W. *J. Am. Chem. Soc.* **1972**, *94*, 1369.

also described in other relationship studies.[25] These anomalies are rationalized in terms of the relatively large changes in π-electron populations at oxygen when OH is converted to O^-, *intramolecular* hydrogen bond stabilizing effects, or the variable contribution of the external stabilization by substituent hydrogen-bond-accepting interactions with water.[22]

It is obvious that solvation effects and the nature of anions play an important role in determining the relative solution acidities of species. The relationship between gas-phase and aqueous acidity described here includes species ranging from those (with strong π-withdrawing substituents, such as $-NO_2$) whose acidities are as strong as the conventional strong organic acids to simple aliphatic alcohols (weak acids) such as methanol or trifluoro-alcohols. The last ones include $-CF_3$ electron-withdrawing groups that exert strong inductive effects. In general, for the anions considered, a substantial part of the negative charge is spread over the entire ion. In the case of weak acids, the negative charge concentration is higher on the O atom of the OH group. The combined resonance and inductive effects of the substituents probably exert a considerable influence in the charge distribution of the anions.[19] Besides, the localized negative charges provide excellent sites for solvation by protic solvents.

3. Summary and Conclusions

Consistent experimental and theoretical investigations of structural effects on the thermodynamical stability of neutral *o-*, *m-*, and *p-* hydroxybenzophenones and their anions (formed by deprotonation of the OH group) are reported and discussed in this work.

The experimental values of the standard molar enthalpy of formation of these species have permitted the estimation of the following results: (i) the stabilizing effect of intramolecular hydrogen bonding in **2H**, (ii) the contribution of a highly stabilized charge-transfer type valence bond structure of *para*-derivative **4H**, and (iii) the effect of the stabilizing *p*-methoxy electron-donating group in the oxybenzone molecule.

The enhanced acidity of **4H** and the higher stability of the corresponding anion, compared with the other isomers, is explained in terms of a greater homogeneity of its anionic charge distribution.

Finally, a relationship has been established between the gas-phase acidity (GA) and pK_a in water solution for phenol derivatives (including hydroxybenzophenones) and some aliphatic alcohols, covering a wide range of GA and pK_a. The attenuation factor found for the acidity in the gas phase is almost 4.5 times larger than in aqueous solvent.

4. Experimental Section

4.1. Purity and Phase Transition Control. DSC Measurements. All samples used in this work were commercially available (Avocado). **2H** and **4H** were purified by sublimation in a Büchi glass oven B-585. **3H** was carefully dried under vacuum at 303 K and used without further purification. Sample purity was checked by differential scanning calorimetry (DSC), using the fractional fusion technique.[26] It showed that the mass fraction impurity of the samples was less than 0.008. From the thermoanalysis study of all of the samples by DSC over the temperature ranges from $T = 260$ K to their melting points (T_{fus}), no phase transition in the solid state were observed. Full details are given in S1 of Supporting Information.

4.2. Static Bomb Combustion Calorimetry. The combustion experiments for **3H** and **4H** were carried out in an isoperibol static *macro*bomb calorimeter, whereas that for **2H** was performed in a *micro*bomb. Detailed description of these methods is found elsewhere.[27] The energy equivalent of the calorimeters, ε(calor), were determined from the combustion of benzoic acid (NIST standard reference sample 39j) with a mass energy of combustion of $-26{,}434 \pm 3\ J\cdot g^{-1}$, under certificate conditions. From 10 calibration experiments, we obtained ε(calor) of $14{,}262.6 \pm 2.5$ and $2108.3 \pm 0.5\ J\cdot K^{-1}$ for macro- and microbomb calorimeters, respectively. The uncertainty quoted is the standard deviation of the mean value. Complementary details are given in S2 of Supporting Information.

4.3. Vapor Pressures and Enthalpies of Sublimation. The standard molar enthalpy of sublimation of **2H** was measured in a high temperature Calvet microcalorimeter, Setaram model HT1000D, by the drop method described by Skinner et al.[28] The measurement procedure and the description of the apparatus have been described in detail by Santos et al.[29] The vapor pressures of **3H** and **4H** as a function of temperature were measured by the combined Knudsen/Quartz crystal effusion apparatus recently developed in Porto.[30] Complementary details of these methods are given in S3 of Supporting Information.

4.4. Ion Gas-Phase Energetics. Gas-phase experiments were carried out in a modified Bruker CMS-47 FT-ICR mass spectrometer equipped with a 4.7 T superconducting magnet and controlled by an IonSpec Omega data station (IonSpec Corp., Irvine, CA).

Determination of Gas-Phase Acidities. Mixtures of **2H** and a reference acid ($A_{ref}H$) of well-known gas-phase acidity were introduced into the high-vacuum chamber. Typical partial pressures were in the range of 2×10^{-8} to 1×10^{-7} mbar. The average temperature of the cell was about 331 K. Isoamyl nitrite (i-$C_5H_{11}NO_2$) containing approximately 20% of methanol was also added. The resonant capture of electrons yielded a mixture of isoamoxide and methoxide anions, which were protonated by **2H** and $A_{ref}H$ yielding exclusively a mixture of $\mathbf{2}^-$ and $A^-{}_{ref}$. The reversible proton transfer, reaction 8, was monitored during 10−20s until an equilibrium state was obtained.

$$\mathbf{2H}(g) + A_{ref}{}^-(g) \rightleftarrows A_{ref}H(g) + \mathbf{2}^-(g) \quad K_p, \Delta_r G^0_m \qquad (8)$$

A Bayard−Alpert ion gauge was used to measure the pressures of the neutral reactants with appropriate correction factors.[31] By definition, the gas-phase acidity (GA(**2H**)) and deprotonation enthalpy ($\Delta_{acid}H^0$(**2H**)) of **2H** are, respectively, the standard Gibbs free energy and enthalpy changes for reaction 9 ($\Delta_r G^0_m(9)$, $\Delta_r H^0_m(9)$)

$$\mathbf{2H}(g) \rightleftarrows \mathbf{2}^-(g) + H^+(g) \quad GA(\mathbf{2H}), \Delta_{acid}H^0(\mathbf{2H}) \qquad (9)$$

Its value can be determined from $GA(A_{ref}H)$ and K_p as follows:

$$GA(\mathbf{2H}) = GA(A_{ref}H) - RT \ln K_p \qquad (10)$$

4.5. Computational Methods. The quantum chemical calculations were carried out using the Gaussian 03 package. The geometries of the compounds under investigation were optimized using the density functional theory (DFT), with the Becke

(25) Wiberg, K. B. *J. Org. Chem.* **2003**, *68*, 875.
(26) (a) Marti, E. E. *Thermochim. Acta* **1973**, *5*, 173. (b) Palermo, E. F.; Chiu, J. *Thermochim. Acta* **1976**, *14*, 1.
(27) (a) Colomina, M.; Jimenez, P.; Roux, M. V.; Turrión, C. *An. Quim.* **1986**, *82*, 126 and references therein. (b) Dávalos, J. Z.; Roux, M. V. *Meas. Sci. Technol.* **2000**, *11*, 1421.
(28) Adedeji, F. A.; Brown, D. L. S.; Connor, J. A.; Leung, M.; Paz-Andrade, M. I.; Skinner, H. A. *J. Organomet. Chem.* **1975**, *97*, 221.
(29) Santos, L.M.N.B.F.; Schröder, B.; Fernandes, O. O. P.; Ribeiro da Silva, M. A. V. *Thermochim. Acta* **2004**, *415*, 15.
(30) Lima, L. M. S. S. PhD. Thesis, University of Porto, **2009**.
(31) Bartmess, J. E.; Giorgiadis, R. M. *Vacuum* **1983**, *33*, 149.

3 parameter and the Lee, Yang, Parr (B3LYP) hybrid functional[32] with 6-311++G(d,p) and 6-311++G(3df,2p) basis set without symmetry restrictions. Harmonic vibrational frequencies were also calculated at the same levels without scaling. The structure of the transition states among conformers were optimized at the 6-311++G(d,p) level, using the methodology QST2 where the transition structure connects the known structures of reactants and products. The TSs were characterized by one imaginary frequency. The levels of theory employed in the present work are expected to provide consistent results for the considered reactions.[33]

Acknowledgment. This work is dedicated to Prof. Manfred Horn M. (Fac. Ciencias, Universidad Nacional de Ingeniería-Lima, Perú). The support of the Spanish MICINN Project CTQ2009-13652 is gratefully acknowledged. C.F.R.A.C. L. thanks FCT and the European Social Fund (ESF) under the third Community Support Framework (CSF) for the award of a Ph.D. Research Grant (SRFH/BD/29394/2006). A.F.L. gratefully acnowledges CNPq and FAPESP (Brazil) for their financial support. Work by A.C. and A.G. was carried out under a JAE-Doc and JAE contracts with CSIC.

Supporting Information Available: DSC measurements; combustion calorimetry, sublimation, and computational results; experimental (XRD) and DFT calculated geometrical parameters; stable dimers of **3H**; total entropy; protonation of the most stable anions at O_1. This material is available free of charge via the Internet at http://pubs.acs.org.

(32) (a) Becke, A. D. *J. Chem. Phys.* **1993**, *98*, 5648. (b) Lee, C.; Yang, W.; Parr, R. G. *Phys. Rev.* **1988**, *B37*, 785.

(33) (a) Raghavachari, K.; Stefanov, B. B.; Curtiss, L. A. *Mol. Phys.* **1997**, *91*, 555. (b) Hehre, W. J.; Radom, L.; Schleyer, P.v.R.; Pople, J. A. *Ab initio Molecular Orbital Theory*; John Wiley & Sons: New York, 1986. (c) Sivaranakrishnan, R.; Tranter, R. S.; Brezinsky, K. *J. Phys. Chem. A* **2005**, *109*, 1621.